

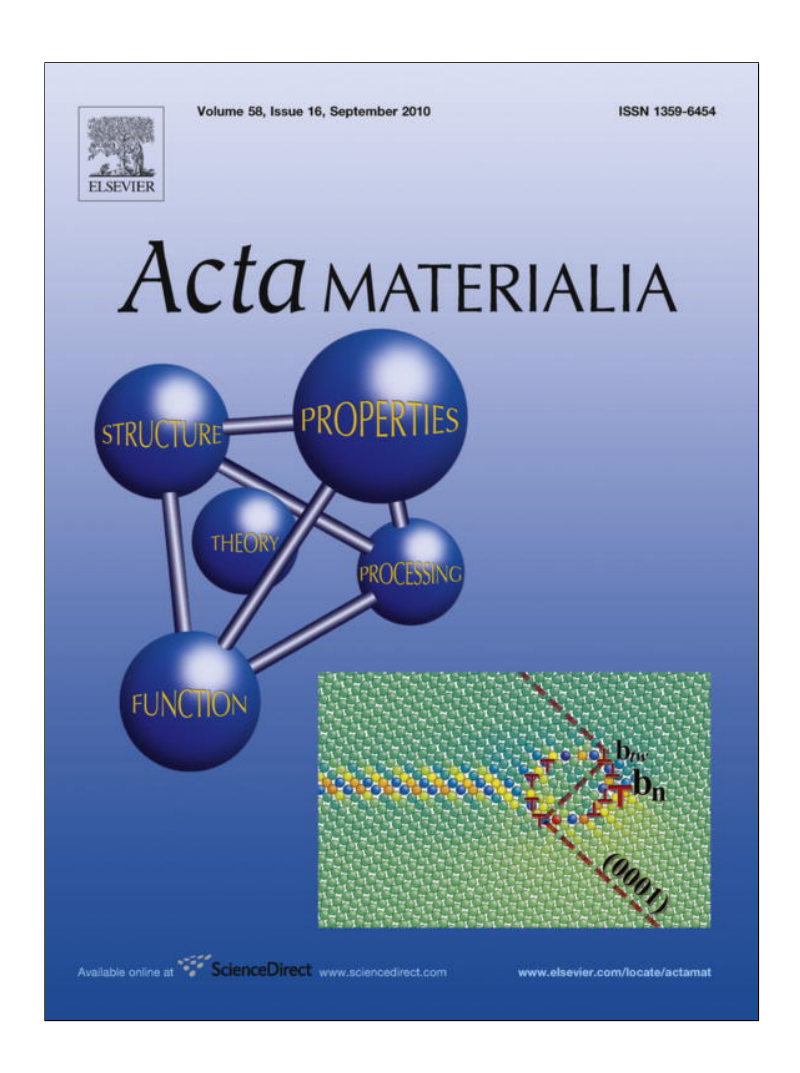
Atom configurations in Pd-Au and Pd-Au-D alloys: A neutron total scattering and Reverse Monte Carlo Study

D.E. Nanu (TU Delft)
M.G. Tucker (ISIS Facility)
W.G. Haije
J.F. Vente
A.J. Böttger (TU Delft)

Published in Science Direct, Acta Materalia 58 (2010) 5502-5510

ECN-W--10-035 August 2010

Provided for non-commercial research and education use. Not for reproduction, distribution or commercial use.



This article appeared in a journal published by Elsevier. The attached copy is furnished to the author for internal non-commercial research and education use, including for instruction at the authors institution and sharing with colleagues.

Other uses, including reproduction and distribution, or selling or licensing copies, or posting to personal, institutional or third party websites are prohibited.

In most cases authors are permitted to post their version of the article (e.g. in Word or Tex form) to their personal website or institutional repository. Authors requiring further information regarding Elsevier's archiving and manuscript policies are encouraged to visit:

http://www.elsevier.com/copyright



Available online at www.sciencedirect.com



Acta Materialia 58 (2010) 5502-5510



www.elsevier.com/locate/actamat

Atom configurations in Pd–Au and Pd–Au–D alloys: A neutron total scattering and Reverse Monte Carlo study

Diana E. Nanu^a, Matthew G. Tucker^b, Wim G. Haije^c, Jaap F. Vente^c, Amarante J. Böttger^{a,*}

^a Department of Materials Science and Engineering, Faculty of Mechanical, Maritime and Materials Engineering, Delft University of Technology, Mekelweg 2, 2628 CD Delft, The Netherlands

^b ISIS Facility, Rutherford Appleton Laboratory, Chilton, Didcot, Oxfordshire OX11 0QX, UK
^c Energy Research Centre of the Netherlands, P.O. Box 1755 ZG Petten, The Netherlands

Received 25 March 2010; received in revised form 5 June 2010; accepted 16 June 2010 Available online 14 July 2010

Abstract

The effect of the alloying elements on the distribution of deuterium in Pd–Au has been investigated by total neutron scattering. The data are analyzed by Reverse Monte Carlo modeling in order to assess the type of interstitial sites occupied with deuterium and how this is correlated with the distribution of the Pd and Au atoms on the host metal lattice. The results show that in Pd–Au alloys deuterium occupies both octahedral and tetrahedral interstitial sites: the overall occupancy of tetrahedral sites increases with increasing Au content and decreasing overall D content. Short-range ordering (SRO) is identified in the D occupancy of interstitial sites in the sample with higher Au content. Indications of SRO and D-induced reorganization in the metal lattice are discussed.

© 2010 Acta Materialia Inc. Published by Elsevier Ltd. All rights reserved.

Keywords: Neutron diffraction; Transition metals; Interstitials; Short-range ordering; RMC modeling

1. Introduction

Supported dense Pd-based membranes with a thickness of several micrometers are considered to be the most suitable option for the production of high-purity hydrogen at reduced costs [1]. Experimental and theoretical studies suggest that addition of specific alloying elements to palladium provides several beneficial effects that lead to Pd-based membranes of higher efficiency and longer operation lifetime. Such beneficial effects are: a reduction of the critical temperature for the transition from the α -metal solid solution to the β -hydride phase, a smaller unit cell volume difference between α and β phase, improved mechanical properties, and an enhanced resistance to surface poisoning, e.g. by sulphur compounds [1,2]. Furthermore, higher

hydrogen solubility and diffusivity for many Pd alloys (e.g. alloys with Ag, Au or Cu) results in higher hydrogen permeability than in Pd itself [2]. The hydrogen solubility and the diffusion mechanism of hydrogen through these membranes are determined by the nature of the specific alloying elements, their concentration and distribution in the metal lattice, through the (local) interaction of the hydrogen atoms with the alloying elements. Information regarding the atomic distribution in the phases formed during hydrogen absorption/desorption in Pd alloys is therefore crucial for understanding and predicting the effect of alloying on the macroscopic hydrogen permeation behavior. These considerations formed our main motivation to investigate the crystal structure of hydrogenated (deuterated) Pd alloys and its relation with the hydrogen desorption characteristics. In a recent paper [3] we discuss desorption characteristics of deuterium from Pd-Au-D alloys in relation with the deuterium site occupancy in the phases formed during deuterium absorption/desorption

^{*} Corresponding author. Tel.: +31 15 278 2243; fax: +31 15 278 6730. E-mail address: A.J.Bottger@tudelft.nl (A.J. Böttger).

in the alloys. The crystal structure information is obtained by neutron diffraction (ND) measurements and analyzed by Rietveld refinement of the Bragg diffraction profiles. The analysis of the ND data showed that the same types of interstitial sites are occupied in the (subcritical) β hydride phases, as well as in the (supercritical) solid solution phases. Only Rietveld refinements including deuterium occupancy of both octahedral (O) and tetrahedral (T) interstitial sites could describe the neutron diffraction data adequately. It was found that with increasing the Au content the occupancy of the O sites decreases while that of the T sites increases [3]. Our results regarding the simultaneous occupation of O and T sites are in agreement with those from theoretical studies on hydrogen in Pd alloys which infer that the occupation of tetrahedral sites may occur depending on the alloying element and its concentration. For example, first-principles studies on hydrogen in Pd-Ag [4-6] and Pd-Au alloys [4,5] suggest that the O site is preferred when most of the neighbors are palladium atoms, while the T site is preferred when the alloying element dominates. First-principles calculations also show that the site occupancy and stability is actually determined by the local atomic arrangement of metal atoms in the nearest neighborhood of the interstitial site [4–8].

Experimental studies supporting the simultaneous occupation of O and T sites and its correlation with the local atomic arrangement on the metal host lattice are, however, not available. Insight into the crystal structure of interstitial alloys can be gained by neutron total scattering measurements, which provide simultaneous information about the average long-range order through the Bragg peaks and the short-range order through the diffuse scattering. The analysis of total scattering data enables one to identify whether deuterium occupancy of the interstitial sites is correlated with the occupancy of the metal host lattice, thereby providing a better understanding of the alloying effect on macroscopic properties such as hydrogen solubility and diffusivity.

This paper presents a detailed analysis of neutron total scattering data measured for Pd-Au-D alloys with different Au and D contents. Deuterium is used instead of hydrogen to avoid a high background due to the incoherent scattering of hydrogen. The system Pd-Au-D is very well suited for neutron diffraction studies since the constituent elements have sufficiently different cross-sections for coherent neutron scattering (i.e. $b_{Pd} = 0.591$ barn, $b_{Au} = 0.763$ barn, $b_{\rm D} = 0.6674$ barn). The data analysis discussed here is based on Reverse Monte Carlo (RMC) modeling, a method that allows to generate structural models consistent with experimental data (i.e. "snap-shots" of the most probable atomic configurations with total scattering characteristics fitting those determined by neutron scattering measurements) and thereby to analyze correlations in the local atomic arrangement. The capability of RMC modeling to reveal information on the local atomic structure and how deviations of the local structure from the average structure given by Rietveld analysis of the Bragg diffraction profiles could explain changes in materials properties has been demonstrated in recent literature [9–12].

2. Experimental

Total neutron scattering measurements were performed on samples comprising pure and deuterated Pd-Au alloys with 10 and 25 at.% Au. Each sample consists of alloy foils 100 µm thick cut as discs of 5 mm diameter and arranged in a cylindrical stack of about 15 mm height with a mass of ca. 3 g. The samples were prepared and handled as previously described [3]: chemical etching using a solution of 2:2:1 H₂SO₄:HNO₃:H₂O, annealing at 1073 K of the pure alloy foils, activation in 0.4 MPa deuterium gas for 15 min at 575 K and degassing at room temperature. The deuterium loading is performed at 303 K and 0.6 MPa D₂. The deuterated samples were placed in a ceramic container sealed in a stainless steel can under deuterium gas at the same pressure as used for deuterium loading. For the neutron total scattering measurements, the specimens were transferred from the ceramic container into a 6 mm thinwalled vanadium can and sealed in air at atmospheric pressure just before the start of each experiment. This was mounted in the sample compartment of the GEM diffractometer at the ISIS spallation neutron source (Rutherford Appleton Laboratory, UK) [13]. All samples were measured for ca. 8 h at room temperature, diffraction patterns being recorded simultaneously by five detector banks positioned at 20 of 154.4°, 91.3°, 63.9°, 35° and 18°, respectively. Background subtraction and data correction were based on measurements of the empty can, empty instrument, and an 8 mm diameter vanadium rod. The data were normalized using standard methods [14] to produce total scattering structure factors and data suitable for Rietveld refinement.

The average structure was refined based on multi-bank data using the Rietveld method as implemented in the GSAS refinement program [15]. Details regarding the refinement procedure are given elsewhere [3]. The average structure determined from Rietveld refinement for each sample was used as starting structure for the RMC modeling.

In brief, RMC modeling (for details see Refs. [14,16,17]) consists of fitting a three-dimensional structural model to experimental data (e.g. total neutron scattering data) via random movements of atoms in the structure model. After each random move a number of structural functions (e.g. G(r), F(Q), defined as given in Ref. [18]) are recalculated based on the new structural model. If the agreement between these calculated functions and the equivalent ones measured experimentally is improved, then the move is accepted; if not, then the move is accepted only with a certain probability. Iterations are continued until the calculated functions agree with the data within certain predefined limits, i.e. the agreement function $\chi^2_{\rm RMC}$ (Eq. (1)) is minimized. As result, by the end of the calculation the atomic configurations that are consistent with the experi-

mental structure factor(s) are available. It should be noted that in the present work the Bragg diffraction data is explicitly used in the RMC fit in addition to the total scattering data and the radial distribution functions. Thus the agreement functions used are defined as in Eq. (1), where the total scattering structure factors, F(Q), and the total radial distribution functions, G(r), are defined as in Ref. [18].

$$\chi_{\text{RMC}}^{2} = \chi_{F(Q)}^{2} + \chi_{G(r)}^{2} + \chi_{\text{Bragg}}^{2}$$

$$= \sum_{j} \frac{\left[F^{\text{calc}}(Q_{j}) - F^{\text{exp}}(Q_{j})\right]^{2}}{\sigma^{2}(Q_{j})}$$

$$+ \sum_{j} \frac{\left[G^{\text{calc}}(r_{j}) - G^{\text{exp}}(r_{j})\right]^{2}}{\sigma^{2}(r_{j})}$$

$$+ \sum_{j} \frac{\left[I^{\text{calc}}(t_{j}) - I^{\text{exp}}(t_{j})\right]^{2}}{\sigma_{I(j)}^{2}(t_{j})}$$
(1)

The RMC refinements were done with the RMCProfile software [19] using structure models of $10 \times 10 \times 10$ crystallographic unit cells, with lattice parameters as obtained by Rietveld refinements.

The unit cells of the initial configurations consist of facecentered cubic (fcc) Pd-Au cells with a given Au content of 10 or 25 at.% and deuterium atoms distributed randomly over the octahedral interstitial sites. The total amount of deuterium in each sample is that determined by Rietveld refinements [3] and confirmed by thermal desorption measurements. The atomic ratios D/(Pd + Au) are 0.52 and 0.33 for $Pd_{90}Au_{10}$ and $Pd_{75}Au_{25}$ alloys, respectively. Vacancies (Vac), i.e. weightless and non-scattering "atoms" with 1.0 Å diameter, were placed in the remaining octahedral and tetrahedral interstitial sites. The following constraints were put on minimum interatomic distances between Pd and/or Au atoms (M) and interstitial (D or $M-M \geqslant 2.0 \text{ Å}, \quad M-D \geqslant 1.5 \text{ Å},$ atoms: $Vac \ge 1.0 \text{ Å}$ $D-D \geqslant 2.3 \text{ A}, \quad D-Vac \geqslant 1.0 \text{ A},$ $Vac \ge 1.0 \text{ Å}$. The cut-off distance between D atoms was taken as 2.3 Å based on the assumption that the generally accepted Switendick criterium [20] regarding the minimum separation distance of 2.1 Å between H atoms in metal hydrides is also fulfilled in Pd-Au deuterides. In the case of Pd-Au-D alloys this implies that the occupation of nearest-neighboring octahedral-tetrahedral sites (at 1.7 Å separation) and nearest-neighboring tetrahedral-tetrahedral sites (at 2.0 Å separation), both smaller than 2.1 Å, are excluded. The validity of this assumption was checked using a cut-off value of 1.5 Å for D–D minimum distance in some additional simulations.

For each investigated sample various initial configurations for the RMC procedure were generated by random swapping of the metal and/or interstitial atoms in the $10 \times 10 \times 10$ supercell. Two types of atomic moves were considered in the RMC fitting procedure, i.e. swap and displacement. In a swap move two atoms (or an atom and a vacancy) on the same sublattice (metal or interstitial) exchange position; such moves allow substitutional disor-

der to be modeled. In a displacement move an atom is translated by a small distance; such moves allow (thermal) displacements to be modeled. Successive RMC steps of swap moves and/or displacement moves were included in the fit procedure, the typical total run time for minimizing the χ^2_{RMC} function being of ca. 125 h for each initial configuration considered. The results presented in this paper are from an average over eight or 10 final RMC configurations independently obtained (by using different starting configurations).

3. Results and discussion

A representative set of experimental and fitted total scattering structure factors, F(Q), and total pair distribution functions expressed as differential correlation functions, D(r), defined as in Refs. [18,19], are shown in Figs. 1 and 2 respectively. Both figures include the data for a pure $Pd_{75}Au_{25}$ alloy and for the deuterated alloy which was loaded at room temperature under 6 bar deuterium gas. The F(Q) and D(r) from RMC calculations are in excellent agreement with the experimental data.

The F(Q) profiles of the D-free and D-containing alloys are similar but the peaks of the deuterated sample are slightly shifted to shorter Q values, consistent with the lattice expansion that occurs upon deuterium loading. The peak shift for the deuterated sample with respect to the D-free sample is also visible in the D(r) profiles given in Fig. 2. Moreover extra peaks appear at small r distances in the D(r) profile of the deuterated sample. These are due to pair correlations including deuterium. At large distances, however, both D-free and D-containing samples have similar D(r) profiles, indicating that no long-range order of D atoms occurs.

For a closer analysis of the nearest neighbors (nn) and next-nearest neighbors (nnn) the total pair distribution functions expressed as total correlation function, T(r), are

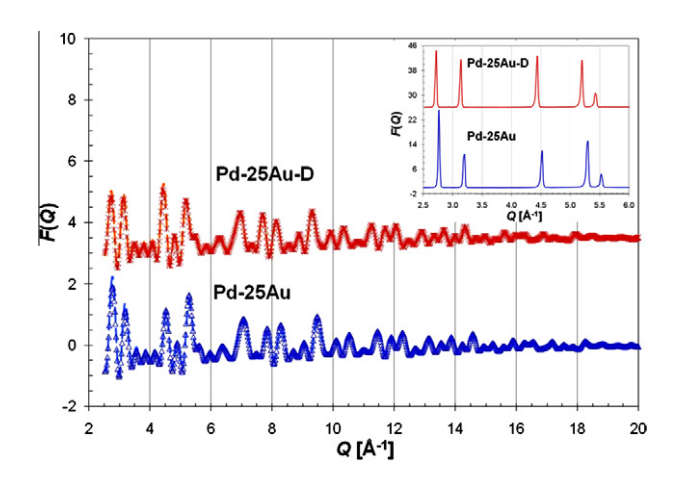


Fig. 1. Representative F(Q) data for $Pd_{75}Au_{25}$ alloy with and without deuterium. The deuterated sample has a D content of 0.33 atomic ratio D/ (Pd + Au). Symbols: experimental data; Lines: RMC fit. Note: the F(Q) data are convoluted with the size of the configuration box. The experimental F(Q) data are given in the inset.

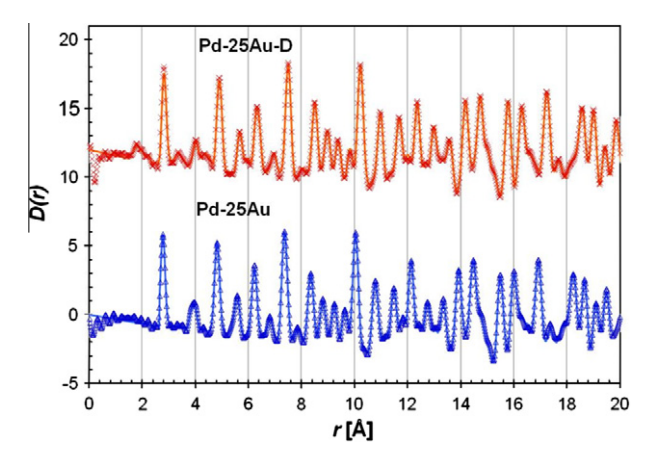


Fig. 2. Differential correlation function data for $Pd_{75}Au_{25}$ alloy with and without deuterium. The deuterated sample has a D content of 0.33 atomic ratio D/(Pd + Au). Symbols: experimental data; lines: RMC fit.

used. The T(r) is defined as in Refs. [18,19]. The T(r) profiles of alloys with different Au content loaded with deuterium under the same conditions (i.e. 6 bar D_2 at 298 K) are compared in Fig. 3. The differences observable in the T(r) profiles of the two alloys, especially at small r distances (i.e. different shape of the "triple" peak centered at 2 Å and of the peak around 3.5 Å) suggest differences in the D occupancy in the two samples. The origin of these peaks was established by analyzing the partial radial distribution functions, $g_{ij}(r)$.

The $g_{ij}(r)$ for D–M pairs (with M being Pd or Au) and D–D pairs calculated by RMC for the optimum configuration for which the best fit of the data is achieved for each of the two samples (i.e. $Pd_{90}Au_{10}-D_{52}Vac_{48}$ and $Pd_{75}Au_{25}-D_{33}Vac_{67}$) are compared in Fig. 4. These $g_{ij}(r)$ values are averages over 10 RMC runs for each sample. The peak positions corresponding to the different D-pairs in a random Pd–Au alloy in which D occupies O and T interstitial positions randomly are indicated by symbols in Fig. 4.

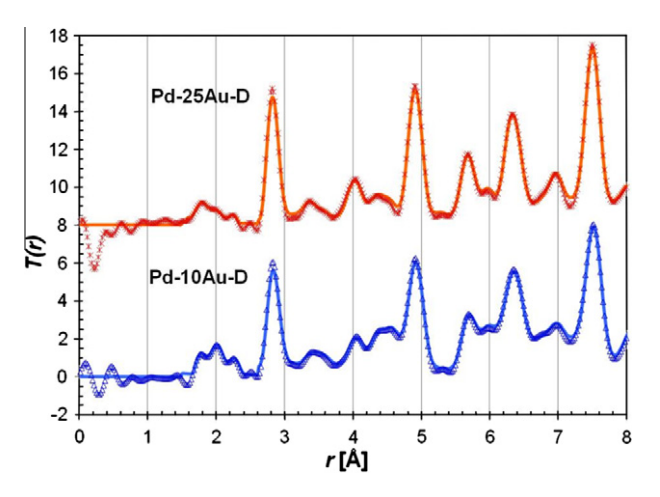


Fig. 3. Total correlation function data for $Pd_{90}Au_{10}$ and $Pd_{75}Au_{25}$ alloys loaded with 6 bar deuterium at 298 K. The D contents correspond to 0.52 and 0.33 atomic ratio D/(Pd+Au) for $Pd_{90}Au_{10}$ and $Pd_{75}Au_{25}$ samples, respectively. Symbols: experimental data; lines: RMC fit.

Although the calculated peaks are rather broad, one can clearly see, especially at small r values, that pairs involving D occupying O sites as well as T sites (i.e. D_O pairs and D_T pairs) occur in both samples. These results indicate the simultaneous occupancy of O and T interstitial sites, which was also evident from the Rietveld refinement of the diffraction data [3]. Note that in each case the initial starting configuration contained all D distributed only over the O sites, thus the T occupancy is the result of RMC fitting the experimental data. The ratio of the area under $g_{ii}(r)$ peaks for D_T pairs with respect to the peaks for D_O pairs is quite different in the two samples considered, suggesting different relative occupancy of T and O sites. In fact, the peak area of D_T pairs (i.e. D_T-M pairs and D_T-D_O and D_T-D_T pairs) is higher in the Pd₇₅Au₂₅-D₃₃Vac₆₇ sample than in Pd₉₀Au₁₀-D₅₂Vac₄₈ (see Fig. 4). This indicates an increase in the fraction of deuterium on T sites with increasing Au content and/or with decreasing the overall D content. Based on Rietveld refinement [3], it was also found that $\sim 50\%$ of D occupies the T sites for the Pd₇₅Au₂₅-D₃₃Vac₆₇ sample while only ~8% of D occupies the T site in the case of Pd₉₀Au₁₀-D₅₂Vac₄₈ alloys. The questions arising now concern the reason for the higher T site occupancy in the Pd₇₅Au₂₅ alloy, which shows lower deuterium solubility than the Pd₉₀Au₁₀ alloy. Is the T site occupancy related to the relative D-Au or D-D interaction? To answer such questions, the $g_{ij}(r)$ s for the D-containing pairs were analyzed in detail.

3.1. Analysis of D-M and D-D pair correlation functions

Fig. 4 shows that not all peaks expected for a random distribution of D atoms (symbols) are observed experimentally and vice versa. Analyzing the $g_{ii}(r)$ s for the D–M pairs in the first coordination shells (i.e. the first group of peaks at r distances between 1.5 and 2.5 Å in Fig. 4A), it can be observed that an extra peak centered at ca. 2.3 Å occurs besides the peaks corresponding to D_T -M (r = 1.74 Å) and D_O-M (r=2 A) pairs. This peak may be attributed to a distorted octahedral occupation occurring as function of the metal surrounding of the O site. In other words, due to the preferential repulsion or attraction of the metal atoms and the D atom, some of the D_O-M bonds are extended while others are shortened. The deformation of the octahedral sites is expected to result in peaks placed around the center of the M–D_O peak (r = 2 A). Depending on how D is shifted from the center of the O site one might expect that the peak at high r values $(r \sim 2.3 \text{ A})$ is bigger than the peak at low r values $(r \sim 1.7 \text{ Å})$; for example, when deuterium is shifted towards one corner of the octahedral it would result in one shorter and five longer D-M distances. Nevertheless, the peak at $r \sim 2.3 \,\text{Å}$ in Fig. 4A does not have a larger area than the peak at $r \sim 1.7$ Å. This is because the peak due to shorter D_O-M pairs overlaps with the peak of D_T –M pairs located at ca. 1.74 Å. In order to evaluate quantitatively the fraction of D_T-M pairs, a fraction of the area of the peak centered at 2.3 Å should

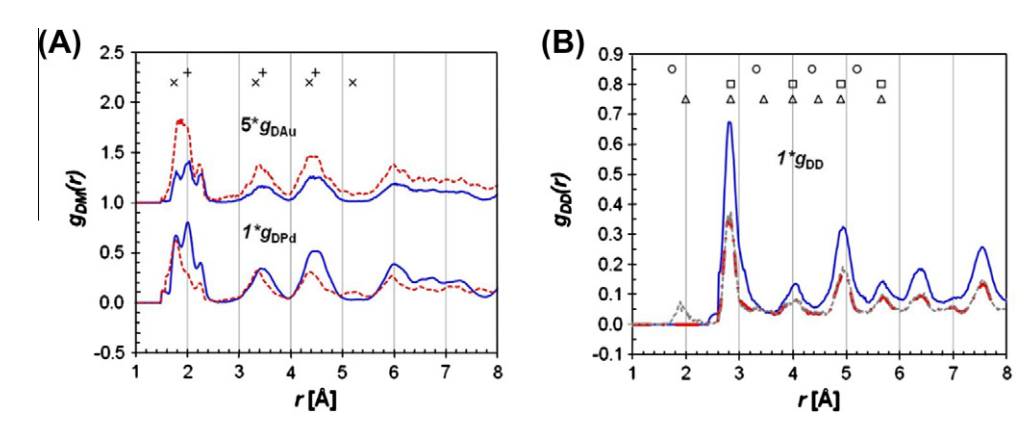


Fig. 4. RMC results of $g_{ij}(r)$ for D–M pairs (A) and D–D pairs (B) for Pd₉₀Au₁₀–D₅₂Vac₄₈ (solid blue line) and Pd₇₅Au₂₅–D₃₃Vac₆₇ (dotted red line). The $g_{ij}(r)$ are concentration scaled partial radial distribution functions ($c_ic_jg_{ij}(r)$). The $g_{DAu}(r)$ are scaled by a factor of five to facilitate comparison with $g_{DPd}(r)$ on the same scale. Symbols indicate the expected peak position of D_0 –M (+), D_T –M (x), D_0 – D_0 (\square), D_0 – D_T (\bigcirc), and D_T – D_T (\triangle) pairs for a random alloy with D distributed randomly over O and T sites. The dotted gray line represents $g_{DD}(r)$ for Pd₇₅Au₂₅–D₃₃Vac₆₇ in the case when a closest approach distance of 1.5 Å was allowed between D atoms. (For interpretation of the references to colour in this figure legend, the reader is referred to the web version of this article.)

Table 1
Average partial coordination numbers in the nearest-neighboring (nn) and next-nearest-neighboring (nnn) coordination shells around an interstitial site calculated from RMC results in comparison with the average partial coordination numbers corresponding to a random distribution of metal atoms around the interstitial sites.

Sample	Coordination shells	D on O site	D on O site		D on T site	
		RMC	Random	RMC	Random	
$Pd_{90}Au_{10}-D_{52}Vac_{48}$						
	$(nn_{\mathrm{DPd}},nn_{\mathrm{DAu}})$	(5.4, 0.6) ±0.3	(5.4, 0.6)	(3.8, 0.2) ±0.1	(3.6, 0.4)	
	$(nnn_{\mathrm{DPd}},nnn_{\mathrm{DAu}})$	(7.2, 0.8) ± 0.5	(7.2, 0.8)	(10.9, 1.1) ±0.4	(10.8, 1.2)	
$Pd_{75}Au_{25}-D_{33}Vac_{67}$						
	$(nn_{\mathrm{DPd}},nn_{\mathrm{DAu}})$	(4.0, 2.0) ±0.2	(4.5, 1.5)	(3.4, 0.6) ±0.3	(3.0, 1.0)	
	$(nnn_{\mathrm{DPd}},nnn_{\mathrm{DAu}})$	(0.0, 8.0) ±0.1	(6.0, 2.0)	(10.3, 1.7) ±0.5	(9.0, 3.0)	

The numbers given in italics indicate the accuracy of determining the coordination numbers, which was estimated using the individual configurations.

be subtracted from the area of the peak at 1.74 Å. Assuming an equal number (upper limit) or five times more of the larger $M-D_{\rm O}$ distances does not significantly change the results for the $M-D_{\rm T}$, as will be discussed later.

The number of Pd and Au atoms in the nearest- and next-nearest-neighboring coordination shells of a D atom occupying an O site and a T site (i.e. partial coordination numbers defined as $n_{ij}(r) = 4\pi q_0 c_j \int r^2 g_{ij}(r) dr$) were determined based on curve fitting. The calculated average partial coordination numbers in the nearest-neighboring (nn) and next-nearest-neighboring (nnn) coordination shells around an O and T interstitial site are summarized in Table 1 in comparison with those corresponding to random distributions. The partial coordination numbers for the random distributions were calculated based on the

probability of combinations, Eq. (2), taking into account the total coordination number in a given shell (N_c) , the number of j atoms in the shell (N_i) and the overall composition of the sublattice expressed in fraction y_i of atom j. The average partial coordination numbers corresponding to a random configuration were obtained by summing the probabilities of occurrence of each type of D-M pair. For example, the average number of Pd atoms nearestneighbors to D on an O site are calculated by summing up the number of D-Pd pairs occurring in each type of octahedrons (i.e. containing 0, 1, 2 ..., or six Pd, and thus contributing with 0, 1, ... and six D–Pd pairs, respectively) multiplied with the probability of finding such type of octahedron (via Eq. (2)). The results are given in Table 1. It should be mentioned that similar occupations were also obtained by integrating the $g_{ii}(r)$ s profiles generated with RMC for random configurations (note that these data are not included in Table 1). This showed that the fitting procedure results in reliable values for occupations.

¹ Lorentzian functions were chosen to describe the peak profiles, the expected peak positions for a random alloy being used as initial peak position parameters. This enables the separation of the overlapping peaks.

$$P_{N_j}(y_j) = \binom{N_C}{N_j} y_j^{N_j} (1 - y_j)^{(N_c - N_j)}$$
 (2)

The data in Table 1 show that the distribution of Pd and Au atoms in the nn and nnn coordination shells around O and T sites occupied by D atoms is about random in the Pd₉₀Au₁₀-D₅₂Vac₄₈ sample. Some short-range ordering occurs in the occupancy of interstitial sites with D in Pd₇₅Au₂₅-D₃₃Vac₆₇. Octahedral sites surrounded only by Au atoms in the *nnn* coordination shell are most favorable for D occupancy amongst the O sites. This is in contrast to the random occupation, for which O sites are on average surrounded by six Pd and two Au atoms in the nnn coordination. This suggests that the local Au concentration in the nnn coordination shell of the O site has a determinant effect on whether the site is favorable or unfavorable for D occupation. In the Pd₇₅Au₂₅–D₃₃Vac₆₇ sample the O sites with 2 nn and 8 nnn Au atoms (RMC average configuration) are more favorable for D than the O sites with 1.5 nn and 2 nnn Au atoms (average for a random configuration). First-principles calculations [4,5] of the hydrogen binding energy on octahedral sites with different metal nn and nnn coordination shells support this statement. Hydrogen binding energies estimated based on Ref. [4] are indeed lower for the observed RMC configurations than those corresponding to the random configurations of nn and nnn Au atoms around the O site. For the estimation of the binding energy, equation (iii) and data from Table 4 of Ref. [4] are used together with the number of Au atoms nn and nnn to an O site from Table 1.

The distribution of Pd and Au atoms in the nn and nnn coordination shells around the T sites depends on the assumption made for the area of the overlapping peak pertaining to the distorted M–D_O occupation: 4.0 Pd and 0.2 Au when assuming equal amounts of r + dr and r - dr distances or 3.8 Pd and 0.2 Au when assuming five longer and one smaller D–M distances in Pd₁₀Au₉₀–D₅₂Vac₄₈. Similarly for Pd₇₅Au₂₅–D₃₃Vac₆₇, this results in 3.5 Pd and 0.5 Au or 3.4 Pd and 0.6 Au.

The distribution of Pd and Au atoms in the nn and nnn coordination shells around the T site occupied by D atoms in Pd₇₅Au₂₅-D₃₃Vac₆₇ also shows some deviations from the average random distribution (see Table 1). There may be some preference for T sites with slightly less nn Au atoms, i.e. 0.6 (or 0.5) Au and 3.4 (or 3.5) Pd instead of the one Au and three Pd as expected for an average random distribution, as well as for T sites with less Au as nnn atoms, i.e. 1.7 Au instead of the three Au expected on average for a random distribution. The distribution of Au atoms in the nn and nnn coordination shells around occupied T sites is about random in the Pd90Au10-D₅₂Vac₄₈, although there may be some preference for T sites with less Au, i.e. sites with 3.8 (or 4.0) Pd and 0.2 (or 0.0) Au as nn are preferred whereas on average 3.6 Pd and 0.4 Au is expected for a random distribution. Thus, some preference for D occupying sites with less Au in nn or nnn shells is found for both samples. Based on chemical

intuition, the fact that the T sites with less Au atoms in the nn and nnn coordination shells are more favorable for D occupancy is not surprising since it is well known that hydrogen is less soluble in Au than in Pd. Also, Mössbauer measurements on Pd-Au-H showed that H atoms did not occupy nearest-neighboring sites of Au [21]. This is also supported by results from first-principles calculations [4,5], which show that, even at low H content, the T sites with no Au atoms as nearest and next-nearest neighbors are indeed more favorable for H binding in Pd-Au alloys with more than 25% Au than the O sites with only Pd in the *nn* and *nnn* surrounding (see Fig. 3b in Ref. [4]). Though the results from these first-principles calculations concern H and not D, it is likely that the T site occupancy will be even more favorable for the heavier isotope because of its lower vibrational energy.

Thus, the occupancy of O and T sites is correlated with the Au concentration in the first and second coordination shells. Moreover, the presence of more Pd and less Au in the nearest and next-nearest coordination shells of a T site makes the site more favorable for D occupation. Based on this observation, one could presume that with increasing Au content the relative occupancy of T sites would decrease. This seems to contradict the previous conclusion drawn based on the relative peak area corresponding to D_O and D_T pairs and the results of the Rietveld refinements. It should, however, be noted that the total D content in the two alloys is also different: the sample with 10 at.%Au contained a larger amount of D than the sample with 25 at.%Au. Due to D-D repulsion, the different D content may also be responsible for the different relative occupancy of the O and T sites in the two alloys. For fcc alloys, Switendick [20] proposed a minimum separation distance between two hydrogen atoms in a metal hydride $(d_0 = 2.1 \text{ Å})$. This implies that an H atom on an O site prevents the occupancy of its eight first nn T sites by another H atom, while an H atom located in a T site prevents the occupancy of its four first nn O sites and six nnn T sites. To check if indeed the assumed minimum separation distance also holds for both alloys investigated, a series of test simulations was performed in which a value of 1.5 Å was used for the minimum D-D interatomic distance. These tests showed that in the case of the Pd₇₅Au₂₅-D₃₃Vac₆₇ alloy some D atoms may occupy sites at distances less than 2.1 Å (i.e. peaks at an r distance of ca. 2 Å in the $g_{DD}(r)$ data represented by the gray line in Fig. 4B indicate the occupancy of adjacent *nn* interstitial sites). Although allowing short D–D correlations does slightly improve the quality of the fit, it is not clear if the initial discrepancy is real or due to transform artifacts in the real space data. Clearly more investigation of the local D-D environment is needed if conclusive conclusion is to be drawn. Nevertheless, the occupation of adjacent nn sites could be due to a favorable metal surrounding of these sites, which makes D-occupation possible regardless the unfavorable D-D repulsion. Our recent first-principles calculations [22] show that the occupation of T sites does indeed become preferable (lower

energy) over the occupation of O sites in Pd₃Au alloys with more than two H atoms per unit cell.

Based on the above discussion, one could conclude that the higher T occupancy in the $Pd_{75}Au_{25}$ – $D_{33}Vac_{67}$ sample results from the combined effect of D–M and D–D interactions, with the former being dependent on the local atomic arrangement of the M atoms in the nearest and next-nearest neighboring shells of the D atoms.

Further analysis of the atomic configurations (Fig. 5) confirms that O and T interstitial sites were simultaneously occupied with D in both investigated alloys. The atomic clouds representing the deuterium distributions in the Pd₉₀Au₁₀-D₅₂Vac₄₈ sample are rather localized around the center of the O and T sites. Those in the Pd₇₅Au₂₅-D₃₃Vac₆₇ sample are well interconnected. This difference in distribution may be taken as an indication of a higher exchange rate of deuterium between adjacent sides, and thus of a higher diffusivity, in the latter sample. The increased exchange rate between adjacent sites in the sample with higher Au content could lead to the higher observed occupancy of T sites. Furthermore, the increased diffusion leads to a tetragonal distortion of the atomic clouds for the sample with 25 at.%Au and could indicate some elastic anisotropy. The higher hydrogen diffusion observed for the sample with higher Au content seems still to be in contradiction with the expected dependence of the (macroscopic) hydrogen diffusivity with the Au content, i.e. a decrease in hydrogen (deuterium) diffusivity is observed experimentally when increasing the Au fraction above 10% [23] and confirmed by theoretical calculations [4,5]. However, both experiments and calculations concern hydrogen diffusivity at very low hydrogen concentrations (close to infinite dilution). At these concentrations, most of the interstitial sites are available for H during diffusion (the diffusion mechanism consists of hydrogen hopping between adjacent interstitial sites, the T sites being considered as intermediary steps in the pathways between O sites [24]). The D content of the samples investigated here is quite high, thus the diffusivity of deuterium is expected to be affected by the availability of unoccupied adjacent interstitial sites. Since 52% of the interstitial sites are already occupied in the Pd₉₀Au₁₀-D₅₂Vac₄₈ alloy, the probability of finding an adjacent unoccupied site is lower than for the Pd₇₅Au₂₅-D₃₃Vac₆₇ alloy, in which only 33% of the sites are occupied. This could explain the differences between shapes in the D distributions in Pd₉₀Au₁₀- $D_{52}Vac_{48}$ alloy (Fig. 5A) and $Pd_{75}Au_{25}-D_{33}Vac_{67}$ alloy (Fig. 5B).

3.2. Analysis of M–M pair correlation functions

The atom distribution on the metal lattice has also been analyzed based on the partial radial distribution functions, $g_{ij}(r)$, for the M-M pairs, with M being Pd and/or Au. The purpose of the analysis is to identify whether the distribution of the M atoms in these solid solution alloys is random or not, and whether changes occur in the occupancy of the

metal host lattice due to the presence of D in the lattice. The $g_{MM}(r)$ s calculated by RMC for the optimum configuration for which the best fit of the data is achieved for each of the samples (i.e. deuterium-free and deuterated alloys) were analyzed in comparison with those corresponding to a random alloy. Only peak positions corresponding to those of random fcc alloys with the same composition are present in the $g_{ii}(r)$ profiles of M-M pairs for both pure alloys and deuterated alloys. The analyzed $g_{MM}(r)$ profiles are the average values of 10 RMC runs for each deuterated sample (i.e. $Pd_{90}Au_{10}-D_{52}Vac_{48}$ and $Pd_{75}Au_{25}-D_{33}Vac_{67}$) and the average values of eight RMC runs for each pure alloy sample (i.e. Pd₉₀Au₁₀ and Pd₇₅Au₂₅). Regarding the peak profiles, it should be remarked that the Au–Au peaks are slightly narrower than the Pd-Pd and Pd-Au peaks in both deuterated samples as well as in both D-free samples. This indicates a narrower distribution of Au-Au bonds close to the average Au-Au bond length due to less thermal motion of Au atoms. The number of Pd and Au atoms in the nearest- and next-nearest-neighboring coordination shells of a given M atom were determined based on curve fitting.² The constitution of the coordination shells determined based on RMC results is compared with those corresponding to random alloys in Table 2. The average partial coordination numbers around a metal atom in the random alloys were calculated in a similar way as those around interstitial atoms.

The data in Table 2 show that, while the number of Pd and Au atoms in the nearest (nn) and next-nearest (nnn) neighboring coordination shells around a Pd atom is random for both the 10 at.%Au and 25 at.%Au alloys, with and without deuterium in the lattice, some deviations from the most probable atomic distribution occur regarding the configuration of the nn and nnn coordination shells around Au atoms. It seems that configurations in which Au is surrounded by more Au atoms as nearest and next-nearest neighbors occur preferentially in the investigated samples (deuterated and pure alloys). This might suggest the presence of some degree of short-range ordering (SRO) in the distribution of Au atoms (i.e. a tendency of Au atoms to cluster). Knowing that RMC is a random method which tend to give the most disordered configurations consistent with the input data, one could conclude that the SRO observed after RMC simulations results most probably from the data. The data in Table 2 indicate that the SRO in the distribution of Au atoms is more pronounced in the sample with lower Au content. Nevertheless, to our knowledge, there is no experimental or theoretical study providing evidence for Au clustering in Pd alloys, such alloys being homogeneous solid solutions at the composition and temperature conditions considered here [25]. There is, however, experimental evidence of ordering in

² Gaussian functions were the most suitable to describe the peak profiles, the expected peak positions for a random alloy being used as initial peak position parameters.

D.E. Nanu et al. | Acta Materialia 58 (2010) 5502-5510

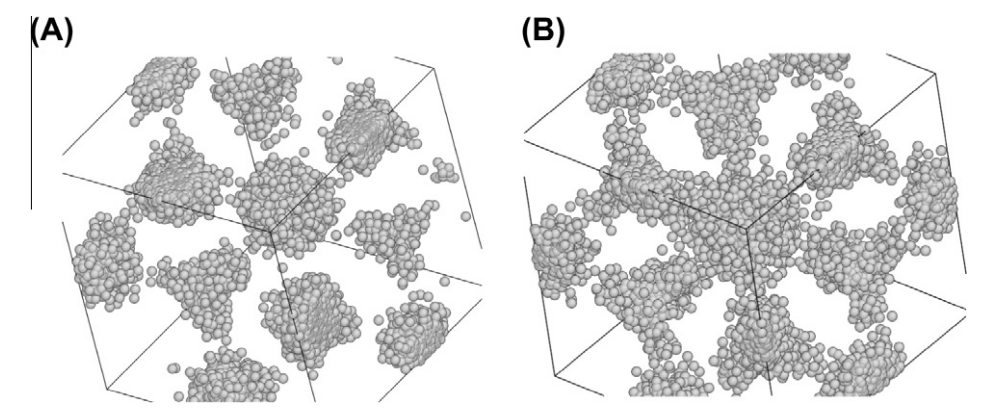


Fig. 5. The distribution of D atoms in Pd-10%Au–D_{0.52} (A) and Pd-25%Au–D_{0.33} (B) as obtained by condensing the atoms of the $10 \times 10 \times 10$ supercell in one unit cell. The view is from [1 1 1] direction.

Table 2 Average partial coordination numbers in the nearest-neighboring (nn) and next-nearest-neighboring (nnn) coordination shells around a metal atom calculated from RMC results in comparison with the average partial coordination numbers corresponding to a random distribution of metal atoms.

Coordination shells	$Pd_{90}Au_{10}$	$Pd_{90}Au_{10}$			Pd ₇₅ Au ₂₅		
	RMC		Random	RMC		Random	
	Without D	With D	Alloy	Without D	With D	Alloy	
$(nn_{\text{PdPd}}, nn_{\text{PdAu}})$	(10.9, 1.1) ±0.2	(10.9, 1.1) ±0.2	(10.8, 1.2)	(9.6, 2.4) ±0.2	(9.6, 2.4) ±0.3	(9.0, 3.0)	
$(\mathit{nnn}_{PdPd},\mathit{nnn}_{PdAu})$	(5.5, 0.5) ±0.5	(5.4, 0.6) ±0.5	(5.4, 0.6)	(4.5, 1.5) ±0.5	(4.8, 1.2) ± 0.4	(4.5, 1.5)	
(nn_{AuPd}, nn_{AuAu})	(8.4, 3.6) ±0.6	(9.9, 2.1) ±0.4	(10.8, 1.2)	(8.8, 3.2) ±0.3	(7.2, 4.8) ± 0.5	(9.0, 3.0)	
$(\textit{nnn}_{AuPd}, \textit{nnn}_{AuAu})$	(4.3, 1.7) ±0.6	(5.1, 0.9) ±0.5	(5.4, 0.6)	(4.2, 1.8) ±0.5	(3.7, 2.3) ± 0.5	(4.5, 1.5)	

The numbers given in italics indicate the accuracy of determining the coordination numbers, which was estimated using the individual configurations.

Pd–Au alloys upon hydrogen permeation and heat treatment under hydrogen [26,27].

Some indication regarding deuterium-induced effects could be obtained comparing the average configurations of the coordination shells of the D-free and deuterated samples with the same Au content. Since the D-free and deuterated samples are made of alloy foils prepared in the same conditions but in different production batches, the interpretation is only qualitative. Nevertheless, some information regarding D-induced effects could be obtained from the data in Table 2, assuming that samples with and without deuterium comprise alloy foils have the same characteristics (i.e. homogeneous composition at microscopic scale, uniform grain size distribution, etc.). For example, regarding the most probable average configuration of the nn and nnn coordination shells around an Au atom, the data in Table 2 show quite different trends in going from the D-free to the deuterated samples for the two alloy compositions. While in the 10 at.% Au samples the configuration becomes closer to the average random configuration in the presence of D in the lattice, the opposite seems to occur for the 25 at.% Au alloys, i.e. the average configuration of the coordination shells around an Au atom contains more Au as nn and nnn atoms in the presence of D than in the D-free sample. This different trend could be probably understood if one considers the previous discussion regarding the distribution of the metal atoms around the occupied interstitial sites. For example, the fact that in the deuterated Pd₉₀Au₁₀ sample the average configuration of the metal atoms around the occupied O and T sites appear to be random implies the requirement that the distribution of the M atoms on the host lattice should be random. This means that, even though in the pure alloy some clustering of Au atoms occurs, this is not the case in the deuterated sample (some reorganizing of the metal host lattice should occur at atomic level). Such a reorganization of the metal lattice under the experimental conditions (low T and P) seems to be impossible, unless the lattice reorganisation had occurred during the activation procedure, which took place under deuterium at 573 K. Experimental evidence [28] that grain boundary diffusion of Pd in Pd-Au alloys is quite significant at temperatures above 500 K could support the above suggestion. Further investigations are required to clarify these issues.

4. Conclusions

Total scattering ND data analyzed by RMC modeling confirm that in Pd-Au alloys deuterium occupies octahedral and tetrahedral interstitial sites, the overall occupancy of tetrahedral sites increasing with increasing Au content and decreasing the overall D content. Short-range ordering is identified in the D occupancy of interstitial sites in the sample with higher Au content (i.e. 25 at.% Au), the sites that appear to be most probable for occupation having a distribution of the metal atoms in the nearest and nextnearest neighboring coordination shells different than the random distribution. For the sample with lower Au content (i.e. 10 at.%) the occupied O and T sites have a random distribution of the metal atoms in the nearest and nextnearest neighboring coordination shells. The local concentration of Au atoms in the nn and nnn coordination shells of the octahedral site has a determinant effect on whether the site is favorable or unfavorable for D binding, i.e. Au repels D, making O sites with only Pd as *nn* atoms and only Au as *nnn* atoms favorable. The higher tetrahedral site occupancy in the deuterated Pd₇₅Au₂₅ sample results from the combined effect of D-M and D-D interactions, with the former being dependent on the local atomic arrangement on the M atoms in the nearest and next-nearest neighboring of the D atoms. A degree of short-range ordering is identified in the distribution of the metal atoms coordinating Au atoms in both D-free and deuterated samples. The presence of D appears to induce some lattice reorganisation; this, however, needs to be confirmed in a future study.

Acknowledgements

The authors gratefully acknowledge ir. W.J. Legerstee and Dr. S.W.H. Eijt from the Department of Radiation, Radionuclides and Reactors of Delft University of Technology for helping with sample preparation. This work is part of a joint research program of the Materials innovation institute (M2i) – the former Netherlands Institute for Metals Research, and the Stichting voor Fundamenteel Onderzoek der Materie (FOM), financially supported by the Nederlandse Organisatie voor Wetenschappelijk Onderzoek (NWO). Further financial support was received through Senter-Novem EOS-LT08008: Consortium Inorganic Membrane Technology. The neutron diffraction

work at ISIS was made possible through an NWO and STFC grant.

References

- [1] Paglieri SN, Way JD. Sep Purif Methods 2002;31:1.
- [2] Sholl DS, Ma YH. MRS Bull 2006;31:770.
- [3] Nanu DE, Legerstee WJ, Eijt SWH, Haije WG, Vente JF, Tucker MG, et al. Acta Mater 2008;56:6132.
- [4] Sonwane CG, Wilcox J, Ma YH. J Phys Chem B 2006;110:24549.
- [5] Sonwane CG, Wilcox J, Ma YH. J Chem Phys 2006;125:184714.
- [6] Lovvik OM, Olsen RA. J Alloys Compd 2002;330-332:332.
- [7] Kamakoti P, Sholl DS. J Membr Sci 2003;225:145;Kamakoti P, Sholl DS. Phys Rev B 2005;71:014301.
- [8] Ke X, Kramer GJ. Phys Rev B 2002;66:184304.
- [9] Tucker MG, Keen DA, Dove MT. Mineral Mag 2001;65:489.
- [10] Tucker MG, Goodwin AL, Dove MT, Keen DA, Wells SA, Evans JSO. Phys Rev Lett 2005;95:255501.
- [11] Goodwin AL, Redfern SAT, Dove MT, Keen DA, Tucker MG. Phys Rev B 2007:76:174114.
- [12] Hull S, Norberg ST, Tucker MG, Eriksson SG, Mohn CE, Stølen S. Dalton Trans 2009:8737.
- [13] Williams WG, Ibberson RM, Day P, Enderby JE. Physica B 1998;241-243:234.
- [14] Dove MT, Tucker MG, Keen DA. Eur J Mineral 2002;14:331.
- [15] Larson AC, Dreele RBV. General structure analysis system (GSAS). LAUR 86-748, Los Alamos National Laboratory; 1994.
- [16] McGreevy RL. J Phys: Condens Matter 2001;13:R877.
- [17] Tucker MG, Dove MT, Keen DA. J Appl Cryst 2001;34:630.
- [18] Keen DA. J Appl Cryst 2001;34:172.
- [19] Tucker MG, Keen DA, Dove MT, Goodwin AL, Hui Q. J Phys: Condens Matter 2007;19:335218.
- [20] Switendick A. Z Phys Chem N F 1979;117:89.
- [21] Wagner F, Karger M, Pröbst F, Schüttler B. In: Jena P, Satterthwaite C, editors. Electronic structure and properties of hydrogen in metals. New York: Plenum; 1983. p. 581–8.
- [22] Talanana M, Nanu DE, Böttger AJ. Internal report. Delft University of Technology, The Netherlands; 2008.
- [23] Ishikawa T, McLellan RB. Acta Metall 1986;34:1825.
- [24] Gillan MJ. J Phys C: Solid State Phys 1986;19:6169.
- [25] Massalski TB, Okamoto H, editors. Binary alloy phase diagrams, vols. 1–3. 2nd ed. Metals Park, OH: ASM International; 1990.
- [26] Lee S-M, Noh H, Flanagan TB, Luo S. J Phys: Condens Matter 2007;19:326222.
- [27] Lee S-M, Flanagan TB, Kim G-H. Scripta Met et Mat 1995;32:827.
- [28] Bukaluk A. Appl Surf Sci 1999;144–145:395.